# Measurement of abdominal visceral fat area of participants in the lung cancer screening with computed tomography

Names of Authors; Syuichiro Yamamoto, Toru Nakagawa, Suzushi Kusano
Institutions of Authors; Hitachi Health Care Center

The metabolic syndrome (MS) is closely associated with coronary artery disease, and the syndrome is suggested to be based on visceral fat accumulation. Therefore, estimating the amount of visceral fat is important. If the additional scan of computed tomography (CT) at the level of umbilicus is performed on participants in the lung cancer screening, we must be able to use this screening more effectively, because screening of not only lung cancer but MS can be done. We measured visceral fat area of these participants using the computer-aided diagnosis (CAD) system which allows automated measurement of visceral fat area, subcutaneous fat area and waist circumference. We evaluated the relationship among the CAD data, body mass index, percentage body fat, blood biochemistry data and blood pressures. We introduce part of our study.

Key words: Computed Tomography(CT)、Metabolic syndrome、Visceral fat area、Computer Aided Diagnosis (CAD)
J Thorac CT Screen 2005;12:200-205

# ＣＴ肺気腫を有する受診者の５年後の喫煙行動と臨床検査の変遷

草野　涼[*1]　中川　徹[*1]　山本　修一郎[*1]　細田　秀一郎[*1]
色川　正貴[*1]　名和　健[*2]

[*1]日立製作所　日立健康管理センタ
（〒317-0076　茨城県日立市会瀬町4-3-16）
e-mail:suzushi.kusano@ibabyo.hitachi.co.jp
[*2]日立総合病院　呼吸器内科

胸部CT検診　Vol.12　No.2　2005

原著

# CT肺気腫を有する受診者の5年後の喫煙行動と臨床検査の変遷

草野　涼[*1]　中川　徹[*1]　山本　修一郎[*1]　細田　秀一郎[*1]
色川　正貴[*1]　名和　健[*2]

【目的】CT肺気腫を有する受診者の、喫煙行動と臨床検査の変遷を観察した。【対象】1998年度の現喫煙者でCT肺気腫を指摘され、5年後にデータ収集できた40名。【方法】検討項目は、1;1年後と5年後の喫煙行動の変容、2;喫煙継続または禁煙達成群に分類した場合のa;体重、b; 白血球数、c; ゲンスラー法による呼吸機能（肺活量、%肺活量、1秒率、1秒量、V25/V50）である。【結果】1年後（1999年度）時点で禁煙したのは6名（15%）で、5年後までに15名（37.5%）が禁煙し25名（62.5%）が喫煙継続中であった。5年後の禁煙達成者の体重は非達成者に比較して有意に増加した。呼吸機能の項目では、V25/V50で禁煙達成者に改善が示唆されたがその他には有意な差はなかった。白血球数は禁煙達成群で改善が示唆された。【考察】調査結果をもとに、今後の研究デザイン構築や禁煙介入プログラムの改善に繋げる。

キーワード：　CT、CT肺気腫、禁煙、呼吸機能検査
J Thorac CT Screen 2005;12:206－210

【はじめに】　胸部CT検査は、肺気腫の存在とその程度を把握するのに非常に有用なのは、疑いないことである。低線量らせんCTを用いた胸部CT検診でも1cm以下の気腫性変化の存在を指摘することが可能であり、臨床的意義を明らかにすべく検討がなされている。[1] [2] [3]

実際の胸部CT検診で見つかるような気腫性変化は、GOLD (The Global Initiative for Chronic Obstructive Lung Disease) [4]のGrade 0に相当するような非常に早期の状態で発見されることがしばしばある。胸部CT検診研究会　肺気腫部会ではこのような画像上確認される気腫性変化を含めてCT画像上で認められる気腫性変化を総じて「CT肺気腫」と定義している。[5]

これまで多くの研究者により、呼吸機能が低下して息切れや慢性的な咳嗽などの臨床症状を伴った肺気腫症例を対象に調査を行われているが、CT画像のみで気腫性変化を指摘され呼吸機能の低下や自覚症状のない早期の症例に対し、経時的に詳細な検討した報告は少ない。

【目的】　我々は、今後のCT肺気腫の研究デザインを確立するためのpre-studyとして、以下のような仮説を立て、CT肺気腫を認めた症例のその後の喫煙行動と呼吸機能の変遷を調査した。

仮説

1;肺気腫を指摘され禁煙の指導を受けた者は、高い禁煙達成率を示す。

2; 禁煙をできた群ではできなかった群に比して、食欲や消化器機能亢進、エネルギー消耗の是正などで体重増加する。

3; 禁煙をできた群ではできなかった群に比して、炎症が改善され白血球数が低下する。

4; 禁煙をできた群ではできなかった群に比して、呼吸機能の低下が軽度である。

調査内容は、98年度に喫煙受診者への介入による、5年後の禁煙率と呼吸機能の変化を観察した。

検討項目は、

[*1]日立製作所　日立健康管理センタ
（〒317-0076　茨城県日立市会瀬町4-3-16）
e-mail:suzushi.kusano@ibabyo.hitachi.co.jp
[*2]日立総合病院　呼吸器内科

1;1年後と5年後の喫煙行動の変容
2;5年後の体重の変容
3;5年後の白血球数の変容
4;5 年後のゲンスラー法による呼吸機能（肺活量・%肺活量・1秒率・1秒量）
である。

【対象と方法】　1998年度にCT肺気腫が確認された受診者のうち、1998年時点での現喫煙の男性受診者で5年後の追跡が可能であった40名を対象とした。

対象者の背景
年齢；平均58.1±5.7歳、
喫煙本数；21.2±4.9本/日
喫煙年数；36.3±6.0年間

CT 肺気腫との診断は、98 年度の初回検診時点での低線量らせん CT にて何らかの低吸収域が確認されたまたは疑われた症例に対して、後日に自施設での高分解能CTでの精密検査は（大動脈弓上縁レベル・気管分岐部レベル・横隔膜上3cmレベル）をもとに行われた。使用した CT 機種は日立メディコ社製 Radix Turbo で、胸部 CT 検診の撮影条件は管電流 50mA 、管電圧 120kVp、スライス厚 10mm、helical pitch2 の低線量らせんCT にて行った。高分解能 CT は、管電流 150mA、管電圧 200kVp、スライス厚 2mm の conventional CT 撮影で行った。

呼吸機能検査は、CHESTAC-11 (Chest corp. Tokyo, JAPAN) または SPIRPSHIFT SP-450A (Fukuda Denshi Ltd. Tokyo, JAPAN)を用いて胸部CT検査に引き続いて行った。修練された技術者により、画面上で flow-volume loops 確認しながら最良のデータを採用した。

受診者には個別に面接し、画像の説明・肺気腫の説明を行い禁煙介入した。1 症例あたりに要する面接時間は、15分程度である。

【結果】　1998年度検診時点で肺気腫を指摘された 40 名の喫煙者のうち、1 年後（1999年度）時点で禁煙していたのは6名（15%）で、5年後（2003年度）に禁煙していたのは15名（37.5%）、喫煙継続中は25名（62.5%）であった。1年後に禁煙達成した者には5年後の再喫煙者はいなかった。（図1）

図1;喫煙行動の変遷

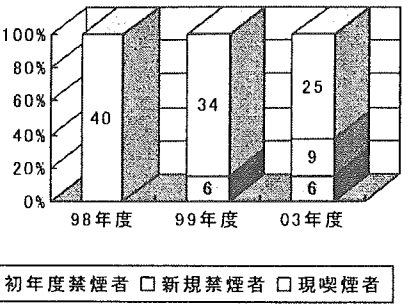


1999 年度までに禁煙しその後禁煙継続できた6名と、2003年度時点で現喫煙者である25 名について、初回受診時(1998 年度)と 5 年経過後（2003年度）の各検査項目の平均は以下の通りである。（表1 a, b)

表1;各検査項目の経時変化
a;1999年度までに禁煙した6名

| | 1998年度 | 2003年度 |
|---|---|---|
| 体重* | 58.2 kg | 66.5 kg |
| 肥満度** | -3.9% | 10.4% |
| 白血球数 | 7450/μl | 5480μl |
| 肺活量 | 3.91 リットル | 3.81 リットル |
| %肺活量 | 109.3% | 109.5% |
| 1秒率 | 76.5% | 70.5% |
| 1秒量 | 3.01 リットル | 2.71 リットル |
| V50/V25 | 3.85 | 3.61 |

肥満度=体重／標準体重
*有意差確率;0.001　**有意差確率;0.002

b;2003年度時点で現喫煙者の25名

| | 1998年度 | 2003年度 |
|---|---|---|
| 体重 | 58.1 kg | 59.2 kg |
| 肥満度 | -1.6% | 0.9% |
| 白血球数 | 7460μl | 6410μl |
| 肺活量 | 3.51 リットル | 3.41 リットル |
| %肺活量 | 101.9% | 101.2% |
| 1秒率 | 75.5% | 72.1% |
| 1秒量 | 2.71 リットル | 2.51 リットル |
| V50/V25 | 3.90 | 4.19 |

体重および肥満度の経時的変化について

は、1999 年度までに禁煙した群と 2003 年度時点で現喫煙者であった群では、前者で有意な体重増加(有意差確率は 0.001)と肥満度の増加（有意差確率は 0.002）が見られた。

白血球数の経時的変化については、1999 年度までに禁煙した群の方がより低下している傾向が見られたが、有意差は無かった。

1999 年度までに禁煙した群と 2003 年度時点で現喫煙者であった群では、肺活量、%肺活量、1 秒率、1 秒量の経時変化に関して有意差は見られなかった。

V50/V25 の経時変化は、平均値では禁煙者で改善し、喫煙者で増悪の傾向が示唆されたが、2 群間での有意差は証明されなかった。

【考察】　過去の我々の報告では、胸部 CT の受診者はその検査結果によらず、1 年あとの禁煙達成率は 30%であったと述べた。今回の調査では、CT 肺気腫を指摘された群の 1 年後の禁煙達成者は 15%であり、想定していたよりも低かった。これには、今回の対象の選出時点に既にいくつものバイアスがあることが原因として考えられるが、その他には肺気腫指摘された直後に禁煙を始めてみたものの 1 年以内に再喫煙してしまったというケースの存在や、もともと CT 肺気腫を呈する集団ではニコチン依存度が高く禁煙に難渋するケースが少なからずいることも予想される。受診者自身に CT 肺気腫の存在を示し禁煙の必要性を説くのみでなく、ニコチン置換療法と行動療法を併用した禁煙プログラムにのせることで、より高い禁煙達成率が期待される。

また、肺気腫の介入後 1 年後以降に禁煙する人は多く見られ、5 年後の禁煙達成率は 37.5%と高いものであった。自らの肺にたばこによる影響が出ていることを視覚的に理解させることは、その人の禁煙に対して高い意識付けになっていると思われる。禁煙に踏み込む、ちょっとの後押しとして機会あるごとに禁煙介入を根気強く継続してゆくことは、禁煙に今一歩踏み込めずに迷っている人や 1 度禁煙したものの再喫煙してしまった人への大きな助けとなると考える。

加えて、今回の調査では 1999 年度までに禁煙した群で有意に体重増加がみられたが、禁煙プログラムには、禁煙後の体重増加防止に関しての指導を含めて行うことが肝要と考える。これにあわせて、脂質代謝や糖代謝などを検討に加え体重増加の健康に与える影響もあわせて研究してゆく。

今回の調査では、1999 年度までに禁煙した群での白血球数は 2003 年度時点で現喫煙者であった群のそれと比較して、低下がみられたが有意差は明らかでなかった。今後、対象数を増やして追試をすることで、有意差がでる可能性がある。一般的に喫煙者の白血球は高い値を示し慢性的な炎症が示唆されるが、禁煙により白血球するが正常に戻るという情報を受診者に伝え、実際の本人のデータでも示すことで、禁煙継続の意志を強めることに役立つものと考える。

1999 年度までに禁煙した群と 2003 年度時点で現喫煙者であった群では、前者の 1 秒率の経時的低下が緩やかと予想したが、2 群間で明らかな差が出なかった。肺気腫は、傍隔壁型肺気腫・小葉中心型肺気腫、汎小葉型肺気腫などの病型があることや、同じように喫煙しておいても個人によってその感受性が異なることがあり、一律の解析が困難となりうる。今回は、1999 年度までに禁煙した群と 2003 年度時点で現喫煙者であった群に分けて検討した。今後更に対象症例を増やし、病型や程度で分類した場合の検討や、非喫煙者や CT 肺気腫を有さない喫煙者を対照とした検討などを加えてゆく必要がある。また、V25/V50 に関して、1999 年度までに禁煙した群では 3.85 から 3.61 と変化し、2003 年度時点で現喫煙者であった群ではと 3.90 から 4.19 と変化した。この両者には有意差を認めなかったものの、前者では改善、後者では悪化することが示唆され、CT 肺気腫の検査項目として重要である可能性がある。その他にも、拡散能検査などで評価も興味深いものであるが、検診（screening study）を運用する上では機器の更新の問題や、時間・労力・資金などのの制限があり今後の課題である。如何に限られた時間・労力・資金・資材を工夫して、肺気腫に必要十分な screening study 行うために、

今回の調査結果をもとに研究デザイン構築や禁煙介入プログラムの改善に繋げる。

【後述】　NICE (Nippon COPD epidemiology study)によると、本邦では530万人の肺気腫を含めたCOPD患者が存在すると推定されているが、1996年に行われた厚生労働省の統計ではCOPD患者数は22万人（男性13万人、女性9万人）とされている。つまり、およそ95%のCOPD患者が診断を受けずに存在することになるが、これらの人への対策としては、COPDとは何かということや呼吸機能の必要性を世間一般に認知させ、呼吸機能検査でのスクリーニングを行うことが重要と考える。一方、胸部CT検査では、呼吸機能検査で異常を認めない人の中にも気腫性変化を有する症例を経験する。かれらに禁煙介入することで、本当に将来のCOPD発症を抑制できるのかをするのかを実証することで、CT肺気腫の臨床意義が明らかになる。

今回の結果を踏まえて、CT肺気腫を指摘された人に対しては、総合的な介入「肺気腫ドック（仮名）」として、肺気腫を含めたCOPDの啓蒙・禁煙介入・呼吸器リハビリを含めた運動処方などを行ってゆく予定である。具体的には、CT肺気腫を指摘された受診者に対して後日に集団教育を行い、ニコチン置換療法と行動療法を併用した禁煙外来の受診を積極的に勧奨する。さらには禁煙後の体重増加を防止するための運動療法・食事療法なども含めた指導を行うことが重要だと考える。

今回のデータには多くのバイアスがあり、また症例数も少なく検証できるものではないと考えられ、研究デザインをたて、cohort studyによって喫煙行動の変化と自覚症状や呼吸機能・CT画像における気腫性変化の程度の経時的な変遷の関係を調査する予定である。

また、CT画像の解析に関しては、CAD（コンピュータ支援診断システム）の開発を行っており、肺気腫の程度を客観的なデータとして得ることができるようになった。[6] [7] このCADの更なる改良を進めるとともに、得られたデータを他の検査データとの相関を引き続き解析して、CT肺気腫の臨床的意義の解明を行ってゆく。CT肺気腫の領域を評価することが、呼吸機能よりも鋭敏に気腫性変化の進行を計る指標になりうる可能性があり、今後の研究結果が期待される。

## 文　献

[1] 山田耕三, 野田和正, 田中利彦, 他: ヘリカルCTによる検診モード画像を用いた肺気腫の早期発見 胸部CT検診 1998; 5: 150-156

[2] 谷野美智枝, 西村正治, 別所智子, 他: 中高年肺癌CT検診における気腫病変の発見頻度 日本呼会誌 2000; 38: 368-372

[3] 名和　健, 中川　徹, 草野　涼, 他：胸部CT検診における肺気腫性変化・喫煙歴, 呼吸機能との関連. 日呼吸会誌　2002；40：468-472

[4] The Global Initiative for Chronic Obstructive Lung Disease: http://www.goldcopd.com/

[5] 胸部CT検診研究会：http://www.thoracic-CT-screening.org

[6] 名和　健, 中川　徹, 草野　涼, 他：「CT肺気腫」定量評価ソフトウエア（riskPointer）の開発. 胸部CT検診　2004；11：104-107

[7] 草野　涼, 中川　徹, 山本　修一郎, 他：胸部CT検診におけるCT肺気腫自動解析装置（riskPointer™）を用いた非喫煙成人肺野の評価. 胸部CT検診　2004；11：108-113

Title

Following up patients who have emphysematous change into the CT screening study.

Names of Authors

Suzushi Kusano[*1], Toru Nakagawa[*1], Shuichirou Yamamoto[*1], Shuichirou Hosoda[*1], Masataka Irokawa[*1], Takeshi, Nawa[*2]

Institutions of Authors

Hitachi Health Care Center, Hitachi ltd. Hitachi Japan [*1]

Hitachi General Hospital, Hitachi Japan [*2]

[Purpose] This is a preliminary study to determine the way of research for the pulmonary emphysematous change, which was pointed out for the first time in the CT screening study. [Materials] 40 cases had the pulmonary emphysematous change who was able to be followed up 6 years later. All of them are current smokers at the base line study. [Methods] Compared with the changing of 1;smoking habit, 2;weight, 3; WBC, 4; pulmonary function test by Gaensler (forced vital capacity = FVC, %FVC, forced-expiratory-volume-for-1second = FEV1.0, FEV1.0 / FCV = FEV1.0% and V25/V50) between base line screening study and 5 years after. [Results] 6 of 40 (15%) cases have done with smoking one year later and total of 15 cases (37.5%) have done. Group of smoking cessations were shown significantly increasing of the weight compared to the group of smokers. There were not significant differences between the any pulmonary function tests. However V25/V50 tended downward in the group of smoking cessations. Besides WBC had tended toward downward in the group of smoking cessations. [Conclusion] Additional prospective study with larger number of cases is necessary to evaluate the clinical meaning of early detecting the pulmonary emphysema in the CT screening study.

Key words: CT screening study, pulmonary emphysema, smoking cessation and pulmonary function tests

J Thorac CT Screen 2005;12:206-210

# Computed tomographic images reflect the biologic behavior of small lung adenocarcinoma: They correlate with cell proliferation, microvascularization, cell adhesion, degradation of extracellular matrix, and K-*ras* mutation

Boming Dong, MD,[a] Masami Sato, MD,[a,b] Akira Sakurada, MD,[a] Motoyasu Sagawa, MD,[a,c] Chiaki Endo, MD,[a] Shulin Wu, MD,[a] Sumitaka Yamanaka, MD,[a] Akira Horii, MD,[d] and Takashi Kondo, MD[a]

GTS

**Background:** We previously reported that the computed tomographic M/L ratio (area of the tumor in the mediastinal computed tomographic image/area of the tumor in the lung computed tomographic image) of small peripheral lung adenocarcinoma is correlated with patient prognosis.

**Methods:** Immunostaining for p53, bcl-2, Ki-67, vascular endothelial growth factor, CD34, matrix metalloproteinase 2, matrix metalloproteinase 9, tissue inhibitor of matrix metalloproteinase 2, and mutation of K-*ras* was assessed in 131 surgically resected, primary peripheral lung adenocarcinomas of 30 mm or less in maximum diameter to clarify the relationship between computed tomographic findings and biologic activities.

**Results:** The numbers of patients with high labeling indexes of Ki-67 and high expression of vascular endothelial growth factor, CD34, matrix metalloproteinase 2, and matrix metalloproteinase 9 in the solid-type group (computed tomographic M/L ratio $\geq$50%) were significantly higher than those in the faint density–type group (computed tomographic M/L ratio <50%; $P = .04$ for Ki-67, $P = .03$ for vascular endothelial growth factor, $P = .0009$ for CD34, $P = .001$ for matrix metalloproteinase 2, and $P = .00001$ for matrix metalloproteinase 9). The number of patients with high levels of CD44v6 or tissue inhibitor of matrix metalloproteinase 2 staining in the faint density–type group was significantly higher than that in the solid-type group ($P = .02$ for CD44v6 and $P = .01$ for tissue inhibitor of matrix metalloproteinase 2). Independent variables capable of predicting computed tomographic M/L ratio included CD34, matrix metalloproteinase 2, matrix metalloproteinase 9, and tissue inhibitor of matrix metalloproteinase 2 ($P = .0093$, $P = .0003$, $P = .0027$, and $P = .01$, respectively; binary logistic regression analysis).

**Conclusions:** Our results suggest that the computed tomographic image of small lung adenocarcinoma is correlated with biologic activities and thus provides possible prognostic information.

From the Department of Thoracic Surgery,[a] Institute of Development, Aging and Cancer, Tohoku University School of Medicine, Sendai, Japan; the Department of Thoracic Surgery,[b] Miyagi Cancer Center, Natori, Japan; the Department of Thoracic Surgery,[c] Kanazawa Medical University, Kanazawa, Japan; and the Department of Molecular Pathology,[d] Tohoku University, Sendai, Japan.

This work was supported in part by the Grant-in-Aid from the Ministry of Education, Culture, Sports, Science, and Technology of Japan.

Received for publication March 1, 2005; revisions received April 29, 2005; accepted for publication May 16, 2005.

Address for reprints: Masami Sato, MD, Department of Thoracic Surgery, Miyagi Cancer Center, 47-1, Medeshima-Shiote-aza-Nodayama, Natori, 981-1293, Miyagi, Japan (E-mail: m-sato@mcc.pref.miyagi.jp).

J Thorac Cardiovasc Surg 2005;130:733-9

0022-5223/$30.00

Copyright © 2005 by The American Association for Thoracic Surgery

doi:10.1016/j.jtcvs.2005.05.013

Recently, the number of patients with small peripheral lung cancer detected by means of computed tomographic (CT) scanning has been increasing. Despite the small size of these tumors, some of these patients die of cancer recurrence. Several factors, including lymph node metastasis, histologic subtype, size of the central fibrosis, and bronchioloalveolar carcinoma (BAC) component, have been proved to be of prognostic importance, but few such factors can be evaluated preoperatively.[1-4] In our previous report we reviewed the CT images of 143 patients with primary peripheral lung adenocarcinoma of 30 mm or less in maximum diameter and classified the patients according to the CT M/L ratio (area

of tumor in the mediastinal CT image/area of tumor in the lung CT image) into a faint density–type group (CT M/L ratio <50%) and a solid-type group (CT M/L ratio ≥50%).[5] As a result, we found that the 5-year survival of patients with faint density–type CT images was significantly better than that of patients with solid-type CT images. Even when the analyses were limited to the patients without nodal involvement, there was also a significant difference between the 2 groups. Multivariate analysis revealed the effect on prognostic influence of the CT M/L ratio on survival to be the second highest after that of the N factor.[5] Thus preoperative classification of patients according to the CT M/L ratio is a simple but powerful predictor of prognosis for patients with small-sized lung adenocarcinoma. Adjuvant treatments, such as chemotherapy and molecular target therapy, are probably necessary for patients with sold-type CT images. Thus it is important to know the mechanism by which CT M/L ratio can be used to predict the prognosis for patients with small-sized lung adenocarcinoma.

The CT M/L ratio might be affected by the pathologic structure of the tumor. BAC components show low cellular density because the tumor cells often extend by mimicking normal alveolar structure. In contrast, fibroblastic proliferation, formation of a central scar, and neovascularization might all contribute to an increase in the value of the CT M/L ratio. None of these factors, however, seems to uniquely predominate in this CT-pathology-survival correlation. On the other hand, p53, Ki-67, bcl-2, CD44v6, vascular endothelial growth factor (VEGF), matrix metalloproteinase 2 (MMP-2), MMP-9, tissue inhibitor of MMP-2 (TIMP-2), and K-*ras*, which were reported to be prognostic factors of small adenocarcinoma, have some influence on histologic structure by affecting cell proliferation, apoptosis, microvascularization, cell adhesion, and the degradation of the extracellular matrix.[6-10] The purpose of this study was to identify the biologic factors that either correlated with the CT M/L ratio or predict the prognosis of small lung adenocarcinoma, so as to clarify the mechanism of the CT-pathology-survival correlation.

## Materials and Methods

### Patients, CT Image Analyses, and Tissue Specimen

In this study, we analyzed resected tumor specimens from 131 patients with primary peripheral lung adenocarcinomas with diameters of 30 mm or less in a period between January 1990 and December 1993. Of the 131 patients, 126 underwent lobectomies, 3 underwent pneumonectomies, and 2 underwent segmental resections combined with systematic hilar and mediastinal node dissection. The CT M/L ratios of tumors were calculated as previously described,[5] and all the patients were classified into one of two groups: a solid-type tumor group and a faint density–type tumor group. The medical records of all the patients were reviewed for clinical and pathologic characteristics. The length of survival was defined as the period from the day of the operation to the last day of follow-up or the date of death from any cause. Thirty 3-$\mu$m–thick sections and two 5-$\mu$m–thick sections were cut from paraffin blocks of the resected tumor for immunohistochemical staining and microdissection, respectively.

### Immunohistochemistry

Immunohistologic staining was performed by the streptoavidin-biotin method (Histofine SAB-PO Kit; Nichirei, Tokyo, Japan), followed by counterstaining with hematoxylin. For antigen retrieval, sections were autoclaved in 10 mmol/L citrate buffer (pH 6.0) before staining. Concentrations of the primary antibodies were optimized by preliminary examinations. Staining without the primary antibody was routinely performed as a negative control. Known immunostaining positive lung adenocarcinoma or squamous cell carcinoma tissue specimens were used as positive controls. The antibodies used in this study were monoclonal p53 antibody (clone DO-7, DAKO, Glostrup, Denmark; diluted 1:50), monoclonal Bcl-2 antibody (clone 124, DAKO, diluted 1:50), monoclonal Ki-67 antibody (clone MIB-1, DAKO, diluted 1:50), monoclonal CD44v6 antibody (clone 2F-10, R&D systems, Minneapolis, Minn; diluted 1:250), monoclonal VEGF antibody (clone R11, IBL, Fujioka, Gunma, Japan; diluted 1:50), monoclonal CD34 antibody (clone QBEnd 10, DAKO, diluted 1:80), monoclonal MMP-2 antibody (clone 8B4, Santa Cruz Biotechnology, Santa Cruz, Calif; diluted 1:200), monoclonal MMP-9 antibody (clone 2C3, Santa Cruz Biotechnology, diluted 1:250), and monoclonal TIMP-2 antibody (clone 3A4, Santa Cruz Biotechnology, diluted 1:250). All the slides were reviewed by three physicians without any knowledge of clinical outcomes or any other clinicopathologic data: two of them (M.S. and A.S.) received formal cytopathologic training. Microscopic evaluation was performed by counting more than 1000 tumor cells in more than 5 randomly selected high-power fields (400×) from different representative parts of the tumor. The Ki-67 labeling index (percentage of nuclear-stained cells) was defined as high when it exceeded the mean value (Figure 1, *a*).[6] The p53[11] staining was defined as positive when more than 10% of the tumor cells showed nuclear staining (Figure 1, *b*). Bcl-2 (Figure 1, *c*),[6] CD44v6 (Figure 1, *d*),[7] MMP-2 (Figure 1, *e*),[12] MMP-9 (Figure 1, *f*),[12] and TIMP-2 (Figure 1, *g*)[12] were defined as positive when more than 10% of the tumor cells showed cytoplasmic staining. For evaluation of VEGF, immunostaining was used to determine the percentage of immunoreactive cells, with the cutoff point for distinguishing specimens with low from high VEGF expression set at 30% of carcinoma cells (Figure 1, *h*). Microvessel density (MVD), as measured by CD34 immunostaining, was determined by using a modification of the technique described by Weidner and colleagues (Figure 1, *i*).[13] The mean MVD was used as a cutoff point for distinguishing between tumors with low and high MVDs.

### Mutation Analysis of K-*ras* at Codons 12 and 13

Two hundred or more tumor cells were laser captured on separate Caps by using a laser capture microdissection microscope (Leica AS LMD; Leica Microsystems, Tokyo, Japan), according to the manufacturer's instructions. DNA was extracted with the QIAamp DNA Mini Kit (50; QIAGEN, Tokyo, Japan), according to the protocol provided by the manufacturer. Exon 1 of the K-*ras* gene was amplified by the nested polymerase chain reaction (PCR) with the first

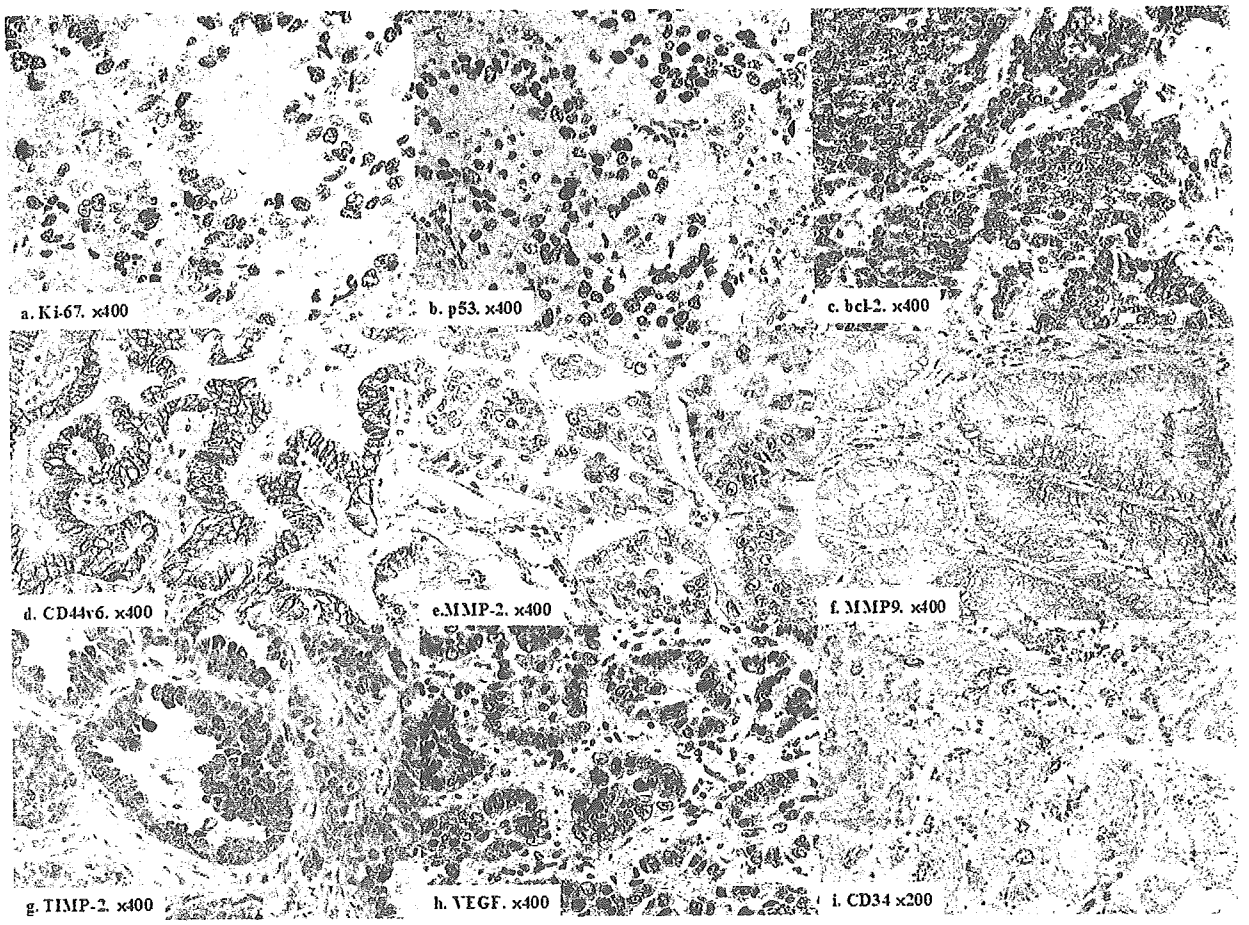


**Figure 1. Immunohistochemical staining of serial sections with various antibodies. Nuclear accumulation of Ki-67 (a) and p53 (b) proteins and cytoplasmic accumulation of bcl-2 (c), CD44v6 (d), MMP-2 (e), MMP-9 (f), TIMP-2 (i), and VEGF (h) proteins are shown in neoplastic cells. (Original magnification 400×.) The CD34-stained endothelial cell clusters were considered as a single countable microvessel, and a tumor area with a high microvessel count is shown in i. (Original magnification 200×.)**

primer set (5′-GACATGTTCTAATATAGTCACAT-3′ and 5′-GTCCTGCACCAGTAATATGC-3′) and the nested primer set (5′-AGGCCTGCTGAAAATGACTG-3′ and 5′-CCTCTATTGTTTG-GATCATATTC-3′), which yielded 205-bp and 125-bp DNA fragments, respectively, covering codons 12 and 13. PCR was carried out in a final 25-$\mu$L reaction mixture containing 4.5 mmol/L Tris-HCl (pH 8.8), 67 mmol/L $(NH_4)_2SO_4$, 6.7 mmol/L $\beta$-mercaptoethanol, 4.5 $\mu$mol/L ethylenediamine tetraacetic acid, 4.5 mmol/L $MgCl_2$, 0.75 pmol each of deoxyribonucleotide triphosphates, 2.5 pmol of each primer, and 0.25 units of Taq DNA polymerase.[14] The mixture was heated at 95°C for 5 minutes and then subjected to 40 PCR cycles (94°C for 30 seconds, 55°C for 30 seconds, and 72°C for 30 seconds). The resulting nested PCR products were run on 4% agarose gels, the 125-bp fragments were isolated, and the DNAs were purified for sequencing reactions. Nucleotides of both the sense and antisense strands were determined by using the BigDye Terminator Cycle Sequencing Ready FS Reaction Kit (Applied Biosystems, Foster City, Calif) and ABI PRISM 310 Genetic Analyzer (Applied Biosystems) by means of methods described previously.[15] This study was approved by the Ethical Committee of Tohoku University School of Medicine and conducted according to the Declaration of Helsinki principles. The appropriate procedure for obtaining informed consent was followed for all the probable individuals participating in the study. Permission for investigations on the old specimens with informed consent that was unavailable during the period of study was obtained from the Ethical Committee of Tohoku University School of Medicine on the basis of a strict evaluation about the essentiality and necessity of the research.

## Statistical Analysis

Survival was calculated by means of the Kaplan-Meier method, and statistical analysis was performed by the log-rank test. The $\chi^2$

test was used to examine group demographic differences. Binary logistic regression analysis was used to identify predictors of CT M/L ratio. The Cox proportional hazards model with a forward stepwise procedure was applied for multivariate analysis. All statistical analyses were performed with version 5.0 of the StatView software package (SAS Institute, Inc, Cary, NC).

## Results

Patient characteristics are summarized in Table 1. There were 53 patients with solid-type tumors and 78 patients with faint density–type tumors. There were no significant differences in sex, age distribution, nodal involvement, or histologic grade between the 2 groups. The 5-year survival of patients with faint density–type images was 81.6%, which was significantly higher than that of patients with solid-type CT images (5-year survival, 63.8%; $P = .004$; Figure 2, *a*).

Positive staining for Ki-67 and p53 protein was detected in the nuclei (Figure 1, *a* and *b*). In all cases the percentage of tumor cells positive for Ki-67 protein ranged from 0.6% to 78.4%, and the mean Ki-67 labeling index was 18.2% ± 16.2%. The expressions of bcl-2, CD44v6, MMP-2, MMP-9, TIMP-2, and VEGF proteins were generally detected in the cytoplasm of tumor cells (Figure 1, *c-h*). The mean MVD stained by CD34 (Figure 1, *i*) for all patients was 59.2 ± 33.8. The numbers of patients with high labeling indexes of Ki-67 and high expressions of VEGF, CD34, MMP-2, and MMP-9 in the solid-type group were significantly greater than those in the faint density–type group ($P = .04$ for Ki-67, $P = .03$ for VEGF, $P = .0009$ for CD34, $P = .001$ for MMP-2, and $P = .00001$ for MMP-9; Table 1). The numbers of patients with high levels of CD44v6 or TIMP-2 staining in the faint density–type group were significantly greater than those in the solid-type group ($P = .02$ for CD44v6 and $P = .01$ for TIMP-2, Table 1). There were no significant differences in the expressions of p53 and bcl-2 proteins between the 2 groups ($P = .64$ for p53 and $P = .10$ for bcl-2, Table 1). The 5-year survivals of patients with high indexes of Ki-67 or low levels of TIMP-2 staining were poorer than those of patients with low indexes of Ki-67 or high levels of TIMP-2 staining ($P = .026$ for Ki-67 and $P = .0005$ for TIMP-2; Figure 2, *b* and *c*). The expressions of VEGF, CD34 (MVD), MMP-2, and MMP-9 proteins seem to be unfavorable prognostic factors (Table 1).

DNA extraction, amplification of K-*ras* by nested PCR, and direct sequencing was successful in 95 cases (43 solid type and 52 faint density type), and K-*ras* mutations were found in 18 (19%) tumors, including 17 mutations on codon 12 (9 GGTGly to TGTCys, 4 GGTGly to AGTSer, and 4 GGTGly to GATAsp) and 1 mutation on codon 13 (GGCGly to GACAsp). The frequency of K-*ras* mutations in the solid-type group was significantly higher than that in the faint density–type group (Table 1). The 5-year survival of patients without a K-*ras* mutation was 0.78, which was significantly better than that of those with a K-*ras* mutation, which was 0.62 ($P = .04$; Figure 2, *d*).

Binary logistic regression analysis revealed the independent variables of significance in predicting CT M/L ratio to be CD34, MMP-9, MMP-2, and TIMP-2 ($P = .0093$, $P = .0003$, $P = .0027$, and $P = .01$, respectively). The multivariate analysis showed N factor, TIMP-2, Ki-67, and tumor size to be significant prognostic factors ($P < .0001$, $P = .0015$, $P = .030$, and $P = .048$, respectively; Table 2).

## Discussion

In this study we found that patients with solid-type tumors had significantly poorer prognoses than those with faint density–type tumors (Figure 2). We also observed that a poor prognosis was associated with high Ki-67 expression and K-*ras* mutation (Figure 2). In multivariate analysis, Ki-67 was proved to be an independent prognostic factor (Table 2). These results were in good agreement with previous reports.[6,11,16-20] In the solid-type group, the number of patients with high labeling indexes of Ki-67, as well as K-*ras* mutation, was significantly higher than that in the faint density–type group (Table 1). Positive correlations between K-*ras* mutation and a high Ki-67 labeling index, a high MVD, a tumor diameter of greater than 20 mm, or low expression of CD44v6 (results not shown) suggest that the K-*ras* mutation affects biologic behaviors, such as cell proliferation, microvascularization, and cell adhesion, and thus the CT M/L ratio in small peripheral lung adenocarcinoma.

Recently, some researchers have reported that increased levels of VEGF expression and new vessel formation were associated with the poorer survival of patients with non–small cell lung cancer.[8,9,21-23] In this study, the numbers of patients with high expression of VEGF and high MVD in the solid-type group were significantly greater than those in the faint density–type group (Table 1). In binary logistic regression analysis, CD34 (MVD) was an independent variable of significance in predicting CT M/L ratio. All these facts indicated that angiogenesis in the solid-type group was much more vigorous than that in the faint density–type group. The newly formed vessels contribute to the increasing CT M/L ratio, as well as to the patient's poor prognosis. Molecular target therapy against tumor-related vessel formation might be adequate for patients with solid-type CT images.

Several recent reports have confirmed that MMP-2 and MMP-9 might predict the outcome of non–small cell lung cancer.[9,24-26] Kumaki and colleagues[27] and Nawrocki and associates[28] have also reported that the expressions of MMP-2, MMP-9, and TIMP-2 differed between atypical adenomatous hyperplasia and BAC or between BAC and invasive adenocarcinoma at the mRNA level or as shown by immunostaining study. Therefore, we investigated the expression of these 3 factors and found that the numbers of patients with high levels of expression of MMP-2 and

**TABLE 1. Clinicopathologic characteristics and summary of immunohistochemical studies and K-*ras* mutations**

| | CT findings | | | | | |
|---|---|---|---|---|---|---|
| | No. of patients | Solid type* | Faint density type† | $\chi^2$ *P* value | 5-y survival | Log-rank test *P* value |
| Sex | | | | .91 | | .40 |
| Male | 61 | 25 | 36 | | 76.4 | |
| Female | 70 | 28 | 42 | | 72.5 | |
| Age (y) | 62.9 ± 9.7 | 62.9 ± 9.6 | 63.0 ± 9.8 | .54 | | .94 |
| Tumor size | | | | .03 | | .01 |
| ≤20 mm | 52 | 15 | 37 | | 83.9 | |
| >20 mm | 79 | 38 | 41 | | 68.8 | |
| Nodal involvement | | | | .09 | | <.00001 |
| N0 | 99 | 36 | 63 | $N^+$ vs $N^-$ | | $N^+$ vs $N^-$ |
| N1 | 7 | 2 | 5 | | | |
| N2 | 25 | 15 | 10 | | | |
| Histologic grade | | | | .015 | | .02 |
| Well | 43 | 13 | 30 | Well vs moderate + poor | | Well vs moderate + poor |
| Moderate | 63 | 29 | 34 | | | |
| Poor | 19 | 5 | 14 | | | |
| *p* stage | | | | .08 | | <.00001 |
| I | 96 | 35 | 61 | Stage I vs stage II-IV | | Stage I vs stage II-IV |
| II | 8 | 2 | 6 | | | |
| III | 26 | 16 | 10 | | | |
| IV | 1 | 1 | 0 | | | |
| p53 | | | | .64 | | .16 |
| Positive | 66 | 28 | 38 | | 67.9 | |
| Negative | 65 | 25 | 40 | | 81.3 | |
| Ki-67 | | | | .04 | | .03 |
| High | 48 | 25 | 23 | | 67.7 | |
| Low | 83 | 28 | 55 | | 79.2 | |
| Bcl-2 | | | | .10 | | .051 |
| Positive | 40 | 12 | 28 | | 82.3 | |
| Negative | 91 | 41 | 50 | | 70.9 | |
| CD44v6 | | | | .02 | | .056 |
| Positive | 80 | 26 | 54 | | 79.4 | |
| Negative | 51 | 27 | 24 | | 66.4 | |
| VEGF | | | | .03 | | .18 |
| Positive | 50 | 26 | 24 | | 66.7 | |
| Negative | 81 | 27 | 54 | | 80.4 | |
| MVD (CD34) | | | | .0009 | | .23 |
| High | 54 | 31 | 23 | | 69.9 | |
| Low | 77 | 22 | 55 | | 77.8 | |
| MMP-2 | | | | .01 | | .82 |
| Positive | 62 | 34 | 28 | | 75.0 | |
| Negative | 69 | 19 | 50 | | 74.2 | |
| MMP-9 | | | | .0001 | | .058 |
| Positive | 93 | 47 | 46 | | 69.0 | |
| Negative | 38 | 6 | 32 | | 87.5 | |
| TIMP-2 | | | | .01 | | .0005 |
| Positive | 90 | 30 | 60 | | 83.3 | |
| Negative | 41 | 23 | 18 | | 55.8 | |
| K-*ras* mutations | | | | .0003 | | .04 |
| Mutant | 18 | 15 | 3 | | 62.2 | |
| Wild type | 77 | 28 | 49 | | 78.4 | |

*CT*, Computed tomography; *VEGF*, vascular endothelial growth factor; *MVD*, microvessel density; *MMP-2*, matrix metalloproteinase 2; *MMP-9*, matrix metalloproteinase 9; *TIMP-2*, tissue inhibitor of matrix metalloproteinase 2. *Solid type: area of the tumor in mediastinal window/area of the tumor in lung window of 50% or greater. †Faint density type: area of the tumor in mediastinal window/area of the tumor in lung window of less than 50%.

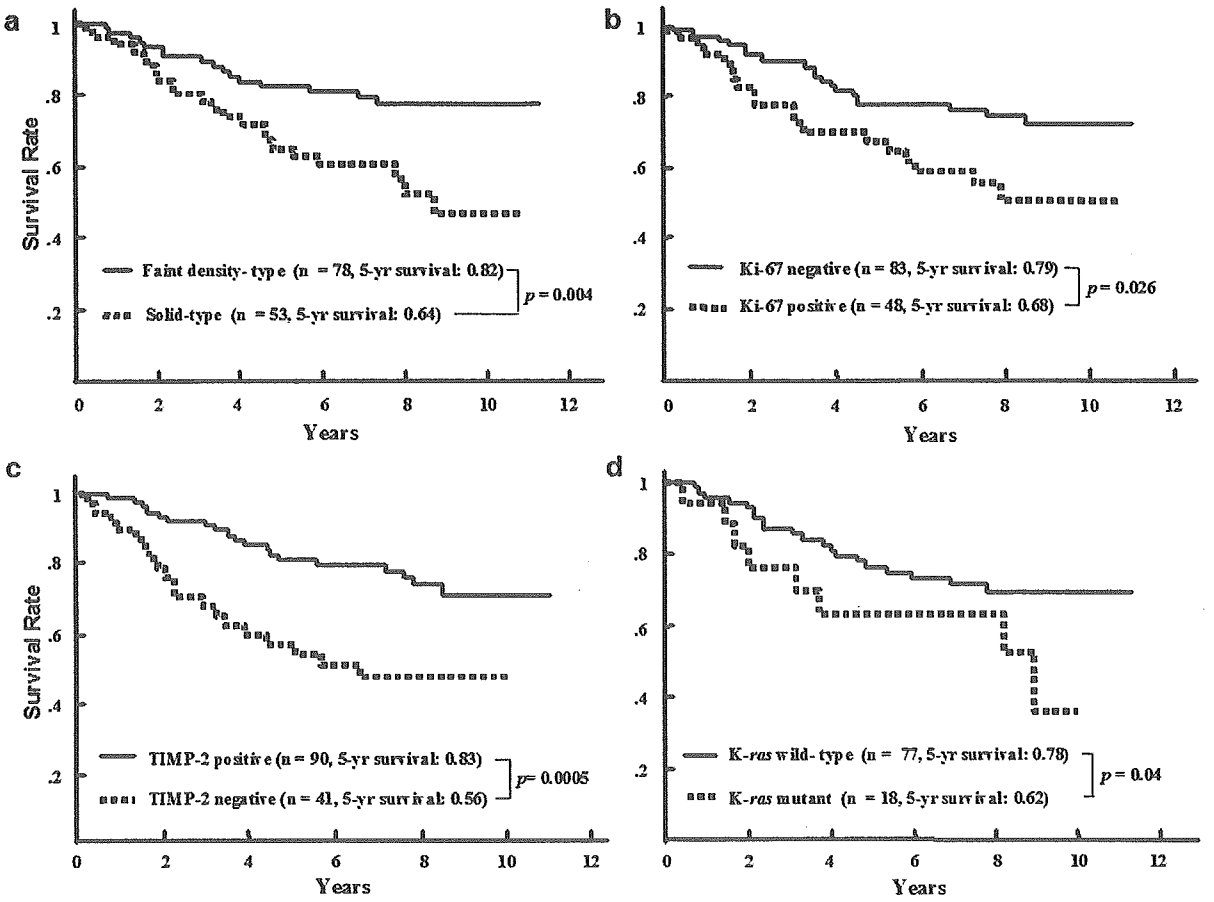


**Figure 2. Survivals of patients with faint density–type images, negative Ki-67 immunostaining, or positive TIMP-2 immunostaining were significantly greater than those of patients with solid-type images, positive Ki-67 immunostaining, or negative TIMP-2 immunostaining ($P = .004$, $P = .026$, and $P = .0005$ in a, b, and c, respectively, by using the log-rank test). The 5-year survival of patients without K-*ras* mutation was 0.78 compared with 0.62 for patients with K-*ras* mutations ($P = .04$ in d).**

MMP-9 or low levels of expression of TIMP-2 in the solid-type group were significantly greater than those in the faint density–type group (Table 1). Furthermore, MMP-2, MMP-9, and TIMP-2 were proved to be the independent variables of significance in predicting CT M/L ratio, and TIMP-2 was proved to be a strong independent prognostic factor of small lung adenocarcinoma both in univariate and multivariate analysis (Tables 1 and 2 and Figure 2, *c*). All these facts suggested that in addition to angiogenesis, degradation of the extracellular matrix was another important factor that affects the CT M/L ratio, and TIMP-2 might have an important role in the development and extension of lung adenocarcinoma. Further research is necessary to explore the mechanisms of TIMP-2, which affect the CT M/L ratio and the prognosis of small lung adenocarcinoma.

**TABLE 2. Multivariate analyses of prognostic factors**

| Variables | Estimated coefficient | SE | *P* value | Relative risk (95% CI) |
|---|---|---|---|---|
| Nodal involvement (N0 vs N1 + 2) | −2.53 | 0.36 | <.0001 | 0.08 (0.04-0.16) |
| TIMP-2 | 1.06 | 0.33 | .0015 | 2.88 (1.50-5.54) |
| Ki-67 | −0.72 | 0.33 | .030 | 0.49 (0.25-0.93) |
| Tumor size (>20 mm vs ≤20 mm) | −0.78 | 0.39 | .048 | 0.46 (0.21-0.99) |

*SE*, Standard error; *CI*, confidence interval; *TIMP-2*, tissue inhibitor of matrix metalloproteinase 2.

In conclusion, tumors with solid-type or faint density–type CT images show significant correlations with factors such as immunostaining of Ki-67, CD44v6, VEGF, CD34 (MVD), MMP-2, MMP-9, TIMP-2, and K-*ras* mutation;

several factors probably affect the promotion of malignant potential in solid-type tumors. To the best of our knowledge, our study is the first to evaluate the correlation of conventional CT images with these biologic factors and to indicate that the CT M/L ratio might provide some information on a tumor's biologic behaviors and might be a prognostic tool for evaluating patients with small peripheral lung adenocarcinoma in the pretreatment period.

We thank Dr Barbara Lee Smith Pierce (University of Maryland University College) for editorial work in the preparation of this article.

## References


1. Suzuki K, Nagai K, Yoshida J, Nishimura M, Takahashi K, Yokose T, et al. Conventional clinicopathologic prognostic factors in surgically resected non–small cell lung carcinoma. *Cancer.* 1999;86:1976-84.
2. Noguchi M, Morikawa A, Kawasaki M, Matsuno Y, Yamada T, Hirohashi S, et al. Small adenocarcinoma of the lung—histologic characteristics and prognosis. *Cancer.* 1995;75:2844-52.
3. Suzuki K, Yokose T, Yoshida J, Nishimura M, Takahashi K, Nagai K, et al. Prognostic significance of the size of central fibrosis in peripheral adenocarcinoma of the lung. *Ann Thorac Surg.* 2000;69:893-7.
4. Higashiyama M, Kodama K, Yokouchi H, Takami K, Mano M, Kido S, et al. Prognostic value of bronchiolo-alveolar carcinoma component of small lung adenocarcinoma. *Ann Thorac Surg.* 1999;68:2069-73.
5. Dong B, Sato M, Sagawa M, Endo C, Usuda K, Sakurada A, et al. Computed tomographic image comparison between mediastinal and lung windows provides possible prognostic information in patients with small peripheral lung adenocarcinoma. *J Thorac Cardiovasc Surg.* 2002;124:1014-20.
6. Ishida H, Irie K, Itoh T, Furukawa T, Tokunaga O. The prognostic significance of p53 and bcl-2 expression in lung adenocarcinoma and its correlation with Ki-67 growth fraction. *Cancer.* 1997;80:1034-45.
7. Ramasami S, Kerr MK, Chapman DA, King G, Cockburn JS, Jeffrey RR. Expression of CD44v6 but not E-cadherin or β-catenin influences prognosis in pulmonary adenocarcinoma. *J Pathol.* 2000;192:427-32.
8. Shibusa T, Shijubo N, Abe S. Tumor angiogenesis and vascular endothelial growth factor expression in stage I lung adenocarcinoma. *Clin Cancer Res.* 1998;4:1483-7.
9. Kodate M, Kasai T, Hashimoto H, Yasumoto K, Iwata Y, Manabe H. Expression of matrix metalloproteinase (gelatinase) in T1 adenocarcinoma of the lung. *Int J Pathol.* 1997;47:461-9.
10. Silini ME, Bosi F, Pellegata Gino Volpato SN, Romano A, Tinelli SNC, Ranzani Enrico Solcia NG, et al. K-*ras* gene mutations: an unfavorable prognostic marker in stage I lung adenocarcinoma. *Virchows Arch.* 1994;424:367-73.
11. Minami K, Saito Y, Imamura H, Okamura A. Prognostic significance of p53, ki-67, VEGF and Glut-1 in resected stage I adenocarcinoma of the lung. *Lung Cancer.* 2002;38:51-7.
12. Michael M, Babic B, Khokha R, Tsao M, Ho J, Pintilie M, et al. Expression and prognostic significance of metalloproteinases and their inhibitors in patients with small-cell lung cancer. *J Clin Oncol.* 1999;17:1802-8.
13. Weidner N, Semple JP, Welch WR, Folkman J. Tumor angiogenesis and metastasis—correlation in invasive breast carcinoma. *N Engl J Med.* 1991;324:1-8.
14. Kimura M, Abe T, Sunamura M, Matsuno S, Horii A. Detailed deletion mapping on chromosome arm 12 in human pancreatic adenocarcinoma: identification of a 1-cM region of common allelic loss. *Genes Chromosomes Cancer.* 1996;17:88-93.
15. Sakurada A, Suzuki A, Sato M, Yamakawa H, Orikasa K, Uyeno S, et al. Infrequent genetic alterations of the PTEN/MMAC1 gene in Japanese patients with primary cancers of the breast, lung, pancreas, kidney and ovary. *Jpn J Cancer Res.* 1997;88:1025-8.
16. Takahashi S, Kamata Y, Tamo W, Koyanagi M, Hatanaka R, Yamada Y, et al. Relationship between postoperative recurrence and expression of cyclin E, p27, and Ki-67 in non-small cell lung cancer without lymph node metastases. *Int J Clin Oncol.* 2002;7:349-55.
17. Demarchi LMMF, Reis MM, Palomino SAP, Takagaki CFTY, Beyruti R, Saldiva PHN, et al. Prognostic values of stromal proportion and PCNA Ki-67, and p53 proteins in patients with resected adenocarcinoma of the lung. *Mod Pathol.* 2000;13:511-20.
18. Huncharek M, Muscat J, Geschwind JF. K-*ras* oncogene mutation as a prognostic marker in non–small cell lung cancer: combined analysis of 881 cases. *Carcinogenesis.* 1999;20:1507-10.
19. Fukuyama Y, Mitsudomi T, Sugio K, Ishida T, Akazawa K, Sugimachi K. K-*ras* and p53 mutations are an independent unfavourable prognostic indicator in patients with non-small-cell lung cancer. *Br J Cancer.* 1997;75:1125-30.
20. Cho JY, Kim JH, Lee YH, Chung KY, Kim SK, Gong SJ, et al. Correlation between K-*ras* gene mutation and prognosis of patients with non–small cell lung carcinoma. *Cancer.* 1997;79:462-7.
21. Folkman J. Angiogenesis in cancer, vascular, rheumatoid and other disease. *Nat Med.* 1995;1:27-31.
22. Yano T, Tanikawa S, Fujie T, Masutani M, Horie T. Vascular endothelial growth factor expression and neovascularisation in non-small cell lung cancer. *Eur J Cancer.* 2000;36:601-9.
23. Inoshima N, Nakanishi Y, Minami T, Izumi M, Takayama K, Yoshino I, et al. The influence of dendritic cell infiltration and vascular endothelial growth factor expression on the prognosis of non–small cell lung cancer. *Clin Cancer Res.* 2002;8:3480-6.
24. Pinto AC, Carvalho EOP, Antonangelo L, Garippo A, Da Silva AG, Soares F, et al. Morphometric evaluation of tumor matrix metalloproteinase 9 predicts survival after surgical resection of adenocarcinoma of the lung. *Clin Cancer Res.* 2003;9:3098-104.
25. Thomas P, Khokha R, Shepherd AF, Feld R, Tsao MS. Differential expression of matrix metalloproteinases and their inhibitors in non-small cell lung cancer. *J Pathol.* 2000;190:150-6.
26. Cox G, Joes JL, Andi A, Waller DA, O'Byrne KJ. A biological staging model for operable non-mall cell lung cancer. *Thorax.* 2001;56:561-6.
27. Kumaki F, Matsui K, Kawai T, Ozeki Y, Yu ZX, Ferrans JV, et al. Expression of matrix metalloproteinases in invasive pulmonary adenocarcinoma with bronchioloalveolar component and atypical adenomatous hyperplasia. *Am J Pathol.* 2001;159:2125-34.
28. Nawrocki B, Polette M, Marchand V, Monteau M, Gillery P, Tournier JM, et al. Expression of matrix metalloproteinases and their inhibitors in human bronchopulmonary carcinomas: quantitative and morphological analyses. *Int J Cancer.* 1997;72:556-64.

Surg Radiol Anat (2005) 27: 94–99
DOI 10.1007/s00276-004-0297-0



**Akira Sakurada · Naoaki Takahashi · Masami Sato**
**Yoshihiro Miyagawa · Hirofumi Matsumura**
**Gen Murakami**

# Are difficulties during transbronchial lung biopsy/brushing through a fiberoptic bronchoscope based on the bronchial anatomy?

Received: 9 December 2003 / Accepted: 4 September 2004 / Published online: 16 December 2004
© Springer-Verlag 2004

**Abstract** Some of the difficulties encountered during transbronchial lung biopsy through a flexible bronchofiberscope are due to anatomical reasons, namely the branching angles of some subsegmental bronchi from their mother bronchi are large, and differences in branching angles during respiration may also be large. This makes insertion of forceps difficult. We have sometimes experienced difficulties reaching the target lesion during a transbronchial approach. Which subsegmental bronchi make transbronchial lung biopsy/brushing difficult, and are such difficulties due to anatomical reasons? To answer these questions, we firstly surveyed 10 bronchologists regarding which five subsegmental bronchi they considered to be the most difficult for transbronchial biopsy/brushing. We then measured the branching angles of subsegmental bronchi in 106 cadaver lungs. Finally, in six volunteers, we also measured differences in branching angles of the subsegmental bronchi between the point of forced inspiration and the point of forced expiration on CT images. According to the survey, left $B^{1+2}c$ was considered to be the most difficult for insertion by nine doctors, followed by bilateral $B^6a$ by seven, right $B^1a$ by five, left $B^3a$ by five and left $B^{1+2}a$ by four. The results of our dissections showed that a branching angle of over 60º was present in more than 10% of specimens in $B^3a$, $B^6a$ and $B^6c$ in the right lung and in $B^{1+2}c$, $B^3a$, $B^6a$ and $B^6c$ in the left lung. In addition, three-dimensional reconstructed images revealed that the angles of some subsegmental bronchi changed during respiration. Inter-individual variations were present in most subsegmental bronchi. The direction of movement of each subsegmental bronchus during respiration varied. In addition, maximum degrees of difference in angles between volunteers were sometimes as much as 80°. In conclusion, branching angles of subsegmental bronchi from their mother bronchi are large in $B^3a$, $B^6a$ and $B^6c$ in the right lung and in $B^{1+2}c$, $B^3a$, $B^6a$ and $B^6c$ in the left lung. Most of these correspond to those which many bronchologists felt to be difficult for insertion. In addition, changes in the angles of subsegmental bronchi during respiration are likely to partially account for difficulties encountered during transbronchial approaches.

**Keywords** Bronchus · Subsegmental bronchus · Transbronchial lung biopsy · Brushing · Bronchoscopy · Anatomy

A. Sakurada
Department of Thoracic Surgery, Institute of Development, Aging and Cancer, Tohoku University, Sendai, Japan

N. Takahashi
Hokkaido Chitose Institute of Rehabilitation Technology, Chitose, Japan

M. Sato (✉)
Department of Thoracic Surgery, Miyagi Cancer Center, Natori, Japan
E-mail: m-sato@mcc.pref.miyagi.jp
Tel.: +81-22-3843151
Fax: +81-22-3811174

M. Sato
47-1, Medeshima, Shiote, aza, Nodayama, 981-1239 Natori, Japan

Y. Miyagawa
Respiratory Physical Therapy, Saiseikai Kumamoto Hospital, Kumamoto, Japan

H. Matsumura · G. Murakami
Department of Anatomy, Sapporo Medical University School of Medicine, Sapporo, Japan

## Introduction

Although it is obvious that pretreatment diagnosis results in benefits to each lung cancer patient, we have sometimes experienced difficulties reaching the target lesion during a transbronchial approach. Thus, an accurate approach through a flexible bronchofiberscope is one of the most important key issues. However, we must sometimes recognize that we have failed to reach the lesion, because we are unable to insert forceps into

the target bronchus, even though we are certain that the tumor is just distal to it. Previously, Shiner et al. [7] reported difficulty in the bronchoscopic approach to the upper lobe of the left lung. Furthermore, according to Nakata et al. [4], bronchi in both lungs present difficulties for insertion. We have also experienced some difficulties during such procedures when the target bronchi were right $B^1$, $B^2$, $B^3$, $B^6$ or left $B^{1+2}$, $B^3$ or $B^6$.

The question we pose here is: Which subsegmental bronchi are difficult for transbronchial lung biopsy/brushing through a fiberoptic bronchoscope? Furthermore, if such difficulties exist, are they due to anatomical reasons and can technological developments help us to overcome them?

In the present study, we attempted to answer these questions in three ways. Firstly, we used a questionnaire to survey experienced bronchoscopists about which subsegmental bronchi present the greatest difficulty for insertion. Secondly, we hypothesized that the branching angle of the subsegmental bronchi originating from the mother segmental bronchus is a critical factor in insertion and biopsy. Finally, we attempted to determine the difference in branching angles during respiration. Thus, we investigated the difference in branching angles between the point of forced inspiration and the point of forced expiration using three-dimensional reconstructed images.

## Materials and methods

A questionnaire for our survey of bronchologists was sent to 10 well-trained bronchoscopists in our prefecture who each had more than 10 years of experience in bronchoscopy. The average number of bronchoscopic procedures performed per year by each bronchoscopist was 150 or more. They were asked to list the five subsegmental bronchi which they felt were most difficult for transbronchial approaches.

### Anatomical study

Out of more than 200 lungs which we prepared for a previous study [3], we selected 106 (54 right, 52 left) according to two criteria:

1. lungs with a clear identification of the segmental bronchi in the upper lobe (conversely, we eliminated lungs with complicated ramifications such as $B^1b + B^2$ in the right lung);
2. lungs without macroscopic pathology, such as tumors including tuberculosis, severe pneumoectasis and adhesive pleuritis.

All 106 lung specimens were removed from 75 cadavers which had been donated for medical education and research and which were fixed by systemic arterial perfusion with 10% formalin solution. They comprised 45 males and 30 females, aged 65–92 years (average 82 years). The lungs were usually fixed at their deep expiratory phase at the time of fixation. The dissection was performed under the naked eye. The branching angle of the outer wall of each subsegmental bronchus was measured. We focused the present measurement on subsegmental bronchi of $B^1$, $B^2$, $B^3$ and $B^6$ in the right lung and $B^{1+2}$, $B^3$ and $B^6$ in the left lung, which have previously been reported as presenting difficulties for insertion.

### CT image analysis for movement of subsegmental bronchi

High-resolution images of six pairs of healthy lungs of six volunteers were obtained and reconstructed. The three-dimensional reconstructed images were used to investigate the difference in the branching angles between the point of forced inspiration and that of forced expiration. We rotated the images to find the most appropriate view for both the mother segmental bronchi and subsegmental bronchi. We measured the branching angles when both the segmental and subsegmental bronchi were in the same plane. The difference in branching angles between the two respiratory phases was presented as the angle calculated by subtracting the angle at the point of forced expiration from that at the point of forced inspiration.

The protocol of the present research project did not include any specific issue that needed approval by the Ethics Committees of our institutions. The present work conformed to the provisions of the Declaration of Helsinki in 1995 (as revised in Edinburgh 2000).

## Results

In terms of the top five most difficult subsegmental bronchi, left $B^{1+2}c$ was chosen by nine doctors, followed by bilateral $B^6a$ by seven, right $B^1a$ by five, left $B^3a$ by five and left $B^{1+2}a$ by four. When asked about the most difficult subsegmental bronchus, left $B^{1+2}c$ was chosen by six doctors, followed by left $B^{1+2}a$ by two, and left and right $B^6a$ by one doctor each.

A branching angle of over 60° was seen in more than 10% of the specimens in $B^3a$, $B^6a$ and $B^6c$ in the right lung and $B^{1+2}c$, $B^3a$, $B^6a$ and $B^6c$ in the left lung (Table 1). In particular, $B^3a$ showed the highest percentages (14/54 or 26% in the right lung and 17/52 or 33% in the left lung), as well as the greatest angle on average of all sites examined (43.9° in the right lung and 48.3° in the left lung). The next greatest angle on average was found in the $B^6$ subsegmental bronchi. The large angles in $B^3a$ included six recurrent subsegmental bronchi with angles from the mother bronchus of more than 90° (2 in the right lung and 4 in the left lung). Another recurrent case was found in $B^6a$ (3 right lungs) and $B^6c$ (1 right lung). Conversely, a small branching angle or linear arrangement between the mother and

**Table 1** Branching angle at which subsegmental bronchi originate from segmental bronchus

| | Right lung bronchi | | | | | | | | |
|---|---|---|---|---|---|---|---|---|---|
| | $B^1a$ | $B^1b$ | $B^2a$ | $B^2b$ | $B^3a$ | $B^3b$ | $B^6a$ | $B^6b$ | $B^6c$ |
| Branching angle at origin (deg; mean ± SD) | 35.4 ± 14.1 | 30.4 ± 11.6 | 31.2 ± 15.0 | 28.3 ± 10.7 | 43.9 ± 21.0 | 20.1 ± 9.0 | 44.8 ± 20.9 | 34.9 ± 14.7 | 42.4 ± 16.1 |
| Percentage of subsegmental bronchi with a branching angle of more than 60 | 7.4% | 1.9% | 3.7% | 0% | 25.9% | 0% | 22.6% | 9.4% | 17.0% |
| | Left lung bronchi | | | | | | | | |
| | $B^{1+2}a$ | $B^{1+2}b$ | $B^{1+2}c$ | $B^3a$ | $B^3b$ | $B^3c$ | $B^6a$ | $B^6b$ | $B^6c$ |
| Branching angle at origin (deg; mean ± SD) | 20.4 ± 12.6 | 24.3 ± 9.9 | 40.0 ± 16.2 | 48.3 ± 21.2 | 25.1 ± 12.7 | 28.2 ± 11.1 | 36.4 ± 14.7 | 23.9 ± 13.3 | 43.5 ± 15.4 |
| Percentage of subsegmental bronchi with a branching angle of more than 60 | 0% | 0% | 11.5% | 32.7% | 1.9% | 0% | 11.5% | 0% | 19.2% |

daughter bronchi was evident in $B^{1+2}a$ (0° or a linear arrangement in 5 lungs and less than 9° in 7 lungs). There was no significant difference in branching angles of subsegmental bronchi between males and females.

Fig. 1 and Fig. 2 show examples of reconstructed images at the point of forced inspiration and the point of forced expiration. We had data for only six healthy volunteers (Tables 2, 3). It was evident that the angles of some subsegmental bronchi changed during respiration. Inter-individual variations were present for most of the values, indicating movement of the subsegmental bronchi. Surprisingly, in most of subsegmental bronchi, the direction of movement of each subsegmental bronchus during respiration varied. For instance, in the right B2a bronchus, the values of angles during respiration were negative in three volunteers but positive in the remaining three. In addition to this, maximum differences in angles between volunteers were sometimes as much as 80 .

## Discussion

Accurate approaches through subsegmental bronchi are very important for achieving high diagnostic yields, because further division of the subsegmental bronchus is sometimes difficult to see with conventional bronchoscopy. Recently, low-dose helical CT screening trials to detect small peripheral lung tumors have shown some promising effects on survival [1, 5, 8, 9]. So, when this screening method becomes widespread, there will be a much greater necessity for an accurate approach to peripheral lesions. Previous investigations of the branching angle along the airway have attempted to formulate general biophysical rules [2, 6]. These efforts, however, concentrated on the distant peripheral parts of the airway and therefore the data cannot be applied to bronchoscopic approaches.

In some previous reports, diagnostic yields were lower when tumors were beyond the right $B^1a$, left $B^{1+2}$, $B^3b$, $B^3c$ or $B^6a$ [4, 7]. Based on the results of our survey, right $B^1a$, $B^6a$ and left $B^{1+2}a,b,c$, $B^3a$ and $B^6a$ appear to be difficult subsegmental bronchi. When we need to reach into the orifices of these subsegmental bronchi, a large reflection of the scope is necessary. However, it is clear that not all subsegmental bronchi are considered to be so difficult. For example, even though a large reflection of the scope is necessary when trying to reach left $B^3b$, none of the bronchologists surveyed listed this subsegmental bronchus as being difficult. Thus, we concluded that the large reflection angle of the scope required during bronchoscopic procedures may be only one of the reasons for difficulties during the procedures.

In our present anatomical studies, we measured the branching angles of subsegmental bronchi from their mother bronchi. During bronchoscopic approaches, the angle of the tip of the bent scope must be changed to coincide with these angles. The results of the present study revealed some possible anatomical limitations during transbronchial approaches through a fiberoptic bronchoscope. To approach segmental bronchi such as $B^1$ and $B^2$ in the right lung or $B^{1+2}$ and $B^3$ in the left lung, a large reflection of the fiberbronchoscope is necessary and then a difficult additional angle is also required to insert the forceps into the subsegmental bronchi.

The large additional angle of the bent scope necessitated by anatomical factors is the main reason for

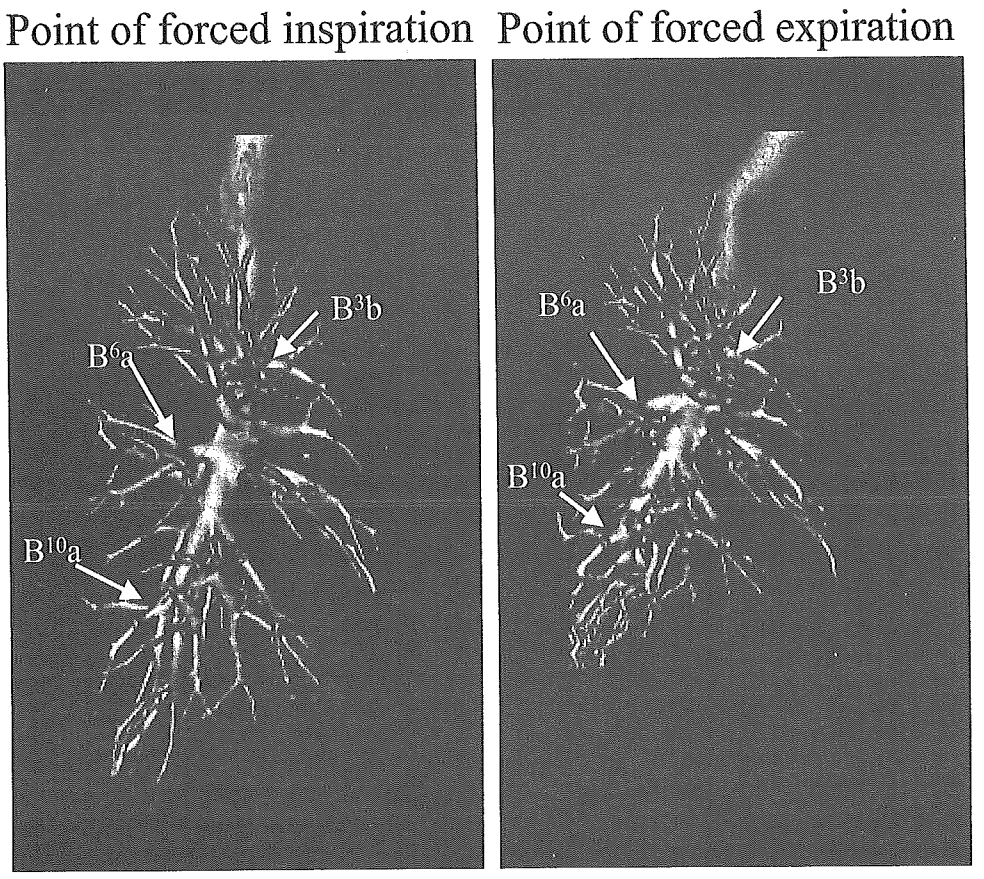


**Fig. 1** Three-dimensional reconstructed images of the right bronchial tree: lateral views

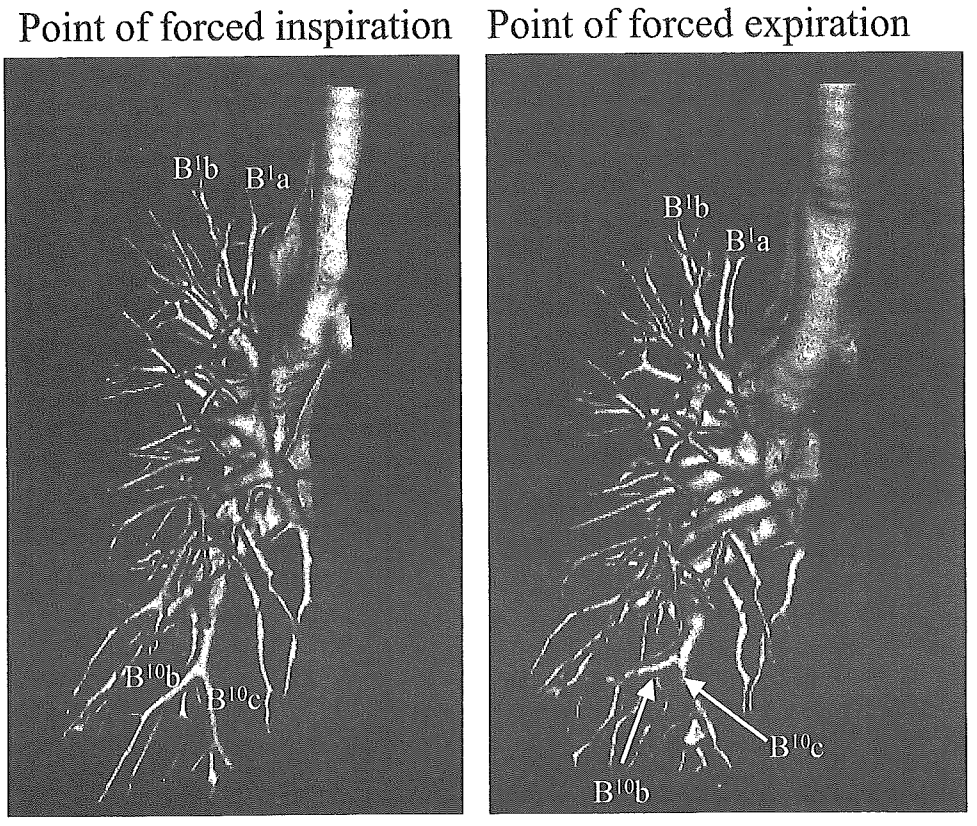


**Fig. 2** Three-dimensional reconstructed images of the right bronchial tree: frontal views

**Table 2** Differences in branching angles in right lung bronchi between the point of forced inspiration and that of forced expiration in six volunteers (*MDD*, maximum degrees of difference in angles between volunteers)

| Bronchi | | Volunteers | | | | | | Mean | MDD |
|---|---|---|---|---|---|---|---|---|---|
| | | 1 | 2 | 3 | 4 | 5 | 6 | | |
| B1 | a | −7 | −15.9 | 11.3 | −7.9 | 39.5 | −31.5 | −1.91 | 71.0 |
| | b | 5.4 | −38.9 | −5.7 | −30.4 | −42.8 | −6.5 | −19.80 | 48.2 |
| B2 | a | −13.1 | −32.1 | 12.4 | 20.6 | 22.1 | −25.5 | −2.60 | 54.2 |
| | b | 23.3 | −6.3 | −5.6 | −8.3 | 21.5 | 38.7 | 10.55 | 47.0 |
| B3 | a | 25.4 | 5.8 | −1.8 | 13.9 | −6.1 | −20.8 | 2.73 | 46.2 |
| | b | −21.7 | −6.8 | −10.8 | 5.4 | −14.8 | 61.1 | 2.07 | 82.8 |
| B4 | a | 15.3 | −3.2 | −10.3 | −13.1 | 0 | 18.9 | 1.27 | 32.0 |
| | b | −10.6 | 10.2 | 15.6 | 16.9 | −1.1 | 33.9 | 10.82 | 44.5 |
| B5 | a | 5.4 | −17.4 | −8.8 | 13.2 | −0.5 | 3.8 | −0.72 | 30.6 |
| | b | −1.3 | −12.8 | −0.8 | −21.5 | −10.8 | −6.7 | −8.98 | 20.7 |
| B6 | a | −18.3 | −19.2 | −15.2 | −3.2 | 5 | −35 | −14.32 | 40.0 |
| | b | 11.3 | −24.9 | −1.5 | −17.2 | −1.6 | −37.5 | −11.90 | 48.8 |
| | c | −10 | −7.6 | −3.9 | 14.9 | 12.7 | −26.5 | −3.40 | 41.4 |
| B7 | a | −21 | 9.4 | −3.7 | −17.9 | −37 | 16.9 | −8.88 | 53.9 |
| | b | −0.6 | −20.4 | −2.9 | 14.6 | −13.6 | −41.1 | −10.67 | 55.7 |
| B8 | a | 17.9 | 8.7 | −13.8 | 0.2 | 6.1 | −0.1 | 3.17 | 31.7 |
| | b | −7.9 | 1.9 | 7.8 | −9.3 | −16.9 | −14.6 | −6.50 | 24.7 |
| B9 | a | −32.5 | −23.3 | −13.2 | −25.7 | −25.6 | −16.9 | −22.87 | 19.3 |
| | b | 21.9 | 8 | −14.5 | −31.2 | −0.7 | 10.9 | −0.93 | 53.1 |
| B10 | a | −31.3 | −8.1 | 2.5 | −28.4 | −20.5 | −39.4 | −20.87 | 41.9 |
| | b | −26.2 | −20 | −28.1 | 4.1 | 19.2 | −31.2 | −13.70 | 50.4 |
| | c | −9.5 | −14 | −4.3 | 0.1 | 9.4 | −14.2 | −5.41 | 23.6 |

**Table 3** Differences in branching angles in left lung bronchi between the point of forced inspiration and that of forced expiration in six volunteers (*MDD*, maximum degrees of difference in angles between volunteers)

| Bronchi | | Volunteers | | | | | | Mean | MDD |
|---|---|---|---|---|---|---|---|---|---|
| | | 1 | 2 | 3 | 4 | 5 | 6 | | |
| B1+2 | a | −27.7 | −11.3 | −8.8 | −23.8 | −17.7 | −11.2 | −16.75 | 18.9 |
| | b | −0.8 | 12.2 | 10.0 | 12.9 | −49.9 | 0.8 | −2.47 | 62.8 |
| | c | 4.6 | −32.4 | −4.1 | −0.8 | 3.6 | −20.5 | −8.27 | 37.0 |
| B3 | a | 13.7 | −18.6 | 9.2 | 5.1 | −17.6 | −45.3 | −8.92 | 59.0 |
| | b | −13.3 | −33.8 | 28.6 | −5.0 | −19.5 | 3.4 | −6.60 | 62.4 |
| | c | 5.0 | −40.8 | −30.9 | −19.5 | −20.4 | −33.6 | −23.37 | 45.8 |
| B4 | a | −35.4 | 8.9 | −15.9 | −5.3 | −18.6 | −3.5 | −11.63 | 44.3 |
| | b | 4.7 | 9.3 | −6.4 | 10.3 | −2.2 | 17.3 | 5.50 | 23.7 |
| B5 | a | −7.8 | −4.6 | 3.0 | −6.3 | −18.9 | −0.5 | −5.85 | 21.9 |
| | b | 4.7 | 13.2 | 20.9 | −2.9 | −9.4 | −1.7 | 4.13 | 30.3 |
| B6 | a | 21.4 | 2.7 | 14.6 | −10.0 | −1.4 | −14.3 | 2.17 | 35.7 |
| | b | −3.2 | 23.8 | −9.7 | −14.5 | 2.0 | −53.0 | −9.10 | 76.8 |
| | c | −6.1 | −33.2 | 23.9 | −6.3 | −17.1 | 16.2 | −3.77 | 57.1 |
| B8 | a | −43.7 | −45.1 | −13.6 | −11.7 | −27.9 | −17.5 | −26.58 | 33.4 |
| | b | 1.6 | −6.3 | 12.1 | −24.6 | −31.6 | −0.1 | −8.15 | 43.7 |
| B9 | a | −11.3 | 4.3 | 2.3 | −8.4 | 11.4 | −36.8 | −6.42 | 48.2 |
| | b | −46.5 | −11.8 | −1.4 | 8.1 | −17.6 | −6.1 | −12.55 | 54.6 |
| B10 | a | 9.2 | −19.5 | 8.3 | −29.5 | −7.2 | −45.9 | −14.1 | 55.1 |
| | b | −16.1 | −33.7 | 10.5 | −2.7 | 3.7 | −13.5 | −8.63 | 44.2 |
| | c | 11.5 | −24.4 | 1.0 | −3.0 | 1.3 | −64.7 | −13.05 | 76.2 |

difficulty of insertion in the subsegmental bronchi, except for left $B^{1+2}a$ and b. From an anatomical point of view, right $B^3a$, $B^6b$, $B^6c$ and left $B^6c$ have large branching angles. These bronchi, however, were not considered to be difficult, which means that there are some discrepancies between anatomical measurements and the impressions of doctors. Both right and left $B^6c$ and $B^6b$, which are not considered to be difficult to enter, have large branching angles from their mother bronchi. However, because the $B^6$ bronchi are short [10], the orifice of $B^6c$ can be easily detected without a large reflection angle of the scope. This may be one reason why it is not felt to be difficult to enter $B^6c$, even though it has a large branching angle. Concerning right $B^3$, our explanations are in relation to the designs of scopes (Fig. 3).

Conversely, left $B^{1+2}a$ and $B^{1+2}b$ are considered by many bronchologists to be difficult subsegmental bronchi, whereas our anatomical study revealed that these subsegmental bronchi have relatively small branching angles, which should indicate easy approaches from their mother bronchi. Another possible explanation

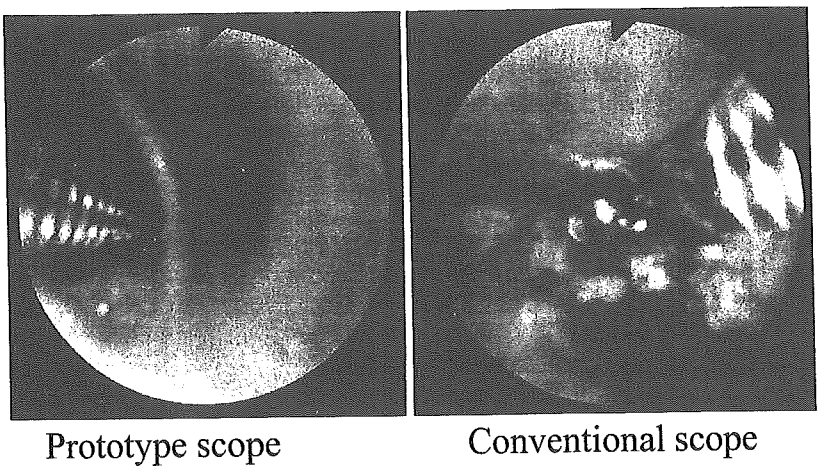


**Fig. 3** Endoscopic view with the Olympus LT30 that has a specially designed left-side channel at the 10 o'clock position (*left*) and that with a conventional scope (*right*)

might be mechanical limitations caused by combinations of forceps and bent scopes. Before left $B^{1+2}a$ and $B^{1+2}b$ can be reached, a large reflection angle of the scope must be made to enter the left upper divisional bronchus for insertion of the forceps. The angles of the tip of the scope might cause resistance to smooth insertion of the forceps, or the forceps themselves may reduce the range of movement of the tip of the scope. Another possible explanation might be mechanical limitations due to the design of the scope. A typical fiberoptic bronchoscope made by the Olympus Company has a channel on the right side for biopsy at the 2 o'clock position in the operator's view. This basic design of the instrument sometimes poses a limitation when approaching a lesion on the left side of the operator's view, especially for taking biopsies in $B^6$, $B^{1+2}$ or $B^3$ in the left lung.

Interestingly, the branching angle of right $B^3a$ is similar to that of left $B^3a$. However, we do not usually experience difficulties when inserting forceps into right $B^3a$, whereas we sometimes fail to insert forceps into left $B^3a$. For this reason, we have developed a specially designed fiberscope with a left-side channel at the 10 o'clock position (Fig. 3). Several groups, including the authors, have reported good results of biopsy in subsegmental levels of $B^1$ or $B^{1+2}$ using this fiberscope (personal communications).

Finally, because we used fixed cadaveric lungs for our anatomical evaluation, there may be some limitations in our study. These lungs were usually fixed at the expiratory point at the time of death, and we obviously could not examine changes in their angles during respiration. Thus, we tried to examine the changes in these angles in six volunteers. Although this is only a preliminary study due to the limited number of volunteers, our results revealed inter-individual variations in changes of angles during respiration. In addition, our results suggest that in some respiratory situations, the angle of the subsegmental bronchi from their mother bronchi increase, and so insertion of forceps would become more difficult. Conversely, in another respiratory phase, it would be easier because the angle would be smaller. In any case, these findings may indicate that insertion of the forceps at different respiratory phases is possible.

We believe that our study has shed light on the difficulties of the bronchoscopic procedure and hope that further investigations, including dynamic movement of the bronchial tree and human engineering science, will provide further insights.

**Acknowledgement** We are grateful to Dr. Mitsuharu Tamakawa of the Division of Diagnostic Radiology at Sapporo Medical University for his kind efforts in preparing the CT images.

## References

1. Henschke CI, McCauley DI, Yankelevitz DF, et al (1999) Early lung cancer action project: overall design and findings from baseline screening. Lancet 354:99–105
2. Horsfield K, Gumming G (1967) Angles of branching and diameters of branches in the human bronchial tree. Bull Math Biophys 29:245–259
3. Koshino T, Murakami G, Sato TJ, et al (2002) Configuration of the segmental and subsegmental bronchi and arteries in the right upper lobe of the human lung with special reference to their concomitant relations and double subsegmental arterial supply. Anat Sci Int 77:64–73
4. Nakata M, Kimura K, Hojyo T, et al (1997) Transbronchial biopsy for peripheral lung lesions. J Jpn Soc Bronchol 19:379–382 (in Japanese with English abstract)
5. Nawa T, Nakagawa T, Kusano S, et al (2002) Lung cancer screening using low-dose spiral CT: results of baseline and 1-year follow-up studies. Chest 122:15–20
6. Sauret V, Goatman KA, Fleming JS, et al (1999) Semi-automated tabulation of the 3D topology and morphology of branching networks using CT: application to the airway tree. Phys Med Biol 44:1625–1638
7. Shiner RJ, Rosenman J, Katz I, et al (1988) Bronchoscopic evaluation of peripheral lung tumors. Thorax 43:887–889
8. Sobue T, Moriyama N, Kaneko M, et al (2002) Screening for lung cancer with low-dose helical computed tomography: Anti-lung Cancer Association Project. J Clin Oncol 20:911–920
9. Sone S, Takashima S, Li F, et al (1998) Mass screening for lung cancer with mobile spiral computed tomography scanner. Lancet 351:1242–1245
10. Takase A. (1959) Morphometrical study of the bronchial tree. Acta Anat Nippon 34:673–702 (in Japanese)